Comparative Catalytic Properties of Ni(OH)$_2$ and NiO Nanoparticles Towards the Degradation of Nitrite (NO$_2^-$) and Nitric Oxide (NO)

Abolanle S. Adekunle[1,*]*, John A.O. Oyekunle*[1]*, Oluwatobi S. Oluwafemi*[2*] *Abiodun O. Joshua*[1]*, Wasiu. O. Makinde*[3]*,Aderemi O. Ogunfowokan*[1]*, Marcus. A. Eleruja*[4]*,* and *Eno E. Ebenso*[5]

[1]Department of Chemistry, Obafemi Awolowo University, Ile-Ife, Nigeria.
[2] Department of Chemistry, Cape-Peninsula University of Technology, P.O Box 652, Capetown 8000. Western Cape, South Africa.
[3]Centre for Energy Research and Development, Obafemi Awolowo University, Ile-Ife, Nigeria
[4]Department of Physics, Obafemi Awolowo University, Ile-Ife, Nigeria
[5]Material Science Innovation & Modelling (MaSIM) Focus Area, Faculty of Agriculture, Science and Technology, North-West University (Mafikeng Campus), Private Bag X2046, Mmabatho 2735, South Africa
[*]E-mail: sadek2k@yahoo.com, aadekunle@oauife.edu.ng, oluwafemi.oluwatobi@gmail.com

Nitrite (NO$_2^-$) and nitric oxide (NO) have been identified as an environmentally hazardous analytes from discharged industrial effluents. Thus in this study, nickel oxide (NiO) and nickel hydroxide (Ni(OH)$_2$) nanoparticles were synthesized using the complexation-precipitation method and their catalytic properties towards NO$_2^-$ and NO investigated. The success of the synthesised nanoparticles was confirmed using characterisation techniques, such as X-ray diffraction (XRD), field emission scanning electron microscopy (FESEM) and the Fourier transformed infrared (FTIR) spectroscopy. The sizes of the synthesized NiO and Ni(OH)$_2$ nanoparticles were estimated to be 5.39 and 5.07 nm respectively. The catalytic behaviour of NiO and Ni(OH)$_2$ nanoparticles towards the oxidative degradation of NO and NO$_2^-$ in acidic and neutral media respectively was studied using UV-Vis spectrophotometer. Result indicated that NiO nanoparticles demonstrated better catalytic properties at different reaction time towards NO$_2^-$ and NO oxidation compared to Ni(OH)$_2$, while NiO and Ni(OH)$_2$ at nano scale showed enhanced catalysis towards the analytes compared with the bulk Ni salt. The bulk Ni salt did not show any sensing properties towards NO$_2^-$. However in NO, the absorbance intensity due to the generation of nitrate (NO$_2^-$) was five times higher in the presence of NiO nanoparticles compared with the bulk Ni salt. The improved catalysis of Ni(OH)$_2$ and NiO nanoparticles in this study was attributed to effective pore sizes and large surface area which expose the analytes to more catalytic site. The nanoparticles are simple to prepare, therefore can be used for the fabrication of a simple, portable, miniaturized nitrite and nitric oxide nanosensor for potential clinical and analytical application.

1. INTRODUCTION

Nickel (II) oxide (NiO) has many of specialized applications including production of alloys, in the ceramic industry to make frits, ferrites and porcelain glazes, for catalysis in both chemical and biological sensors [1-3], and in energy devices such as batteries and supercapacitors [4-6]. NiO is very useful in ceramic and glass as colouring agent. Nano-sized NiO is a good catalyst in the process of decomposition, synthesis, transformation of organics such as gasoline hydrogenation cracking, hydrocarbon conversion and heavy oil hydrogenation. NiO has been used as catalyst to remove CH$_4$, N$_2$, cyanide, and helping to dissolve NO$_X$ [7]. It also serves as a light catalyst to degrade acid red, and excellent catalyst in dealing with organic dye wastewater. NiO is an important gas sensor material in recent years. It was used as formaldehyde, CO and H$_2$ sensors [8]. NiO was also a component in the Nickel-iron battery, also known as the Edison Battery, and is a component in fuel cells [9].

On the other hand, nickel hydroxide (Ni(OH)$_2$) is an insoluble compound which has been extensively studied in the battery industry due to its reactivity in redox processes, electrocatalysis and electrochromic electrodes. In particular, as a good capacitor, it is frequently used for the storage of electrochemical energy [10]. Nickel Hydroxide is generally available in most volumes. Ultra high purity and high purity compositions improve both optical quality and usefulness as scientific standards. Nanoscale elemental powders and suspensions provide large surface area for catalysis [11-13].

Environmentally important molecules such as nitrites (NO$_2^-$) and nitric oxide (NO) have attracted the attention of analytical chemists and electrochemist in recent times. The nitrite ion is an intermediate species in the nitrogen cycle, resulting from the oxidation of ammonia or from reduction of nitrate. It is used as an additive in some types of food and its occurrence in soils, waters, foods and physiological systems is prevalent leading to oxygen depletion to the tissues [14]. Since nitrite is a nutrient and excretion product of phytoplankton [15], its detection and quantification in oceans, rivers and drinking water is of importance in environmental monitoring. Nitrite has also been implicated in the global nitrogen and carbon cycles with resulting effects on climate [16,17].

Nitric oxide (NO) on the other hand is a free radical and an important intermediate in the chemical industry, which finds its way to the environment through industrial effluents. Nitric oxide is also a by-product of combustion of substances in the air, as in automobile engines, fossil fuel power plants and is produced naturally during the electrical discharges of lightning in thunderstorms. In mammals including humans, NO is an important cellular signaling molecule involved in many physiological and pathological processes. It is a powerful vasodilator with a short half-life of a few seconds in the blood. Low levels of nitric oxide production are important in protecting organs such as the liver from ischemic damage. Nitric oxide is rapidly oxidized in air to nitrogen dioxide. Despite being a simple molecule, NO is an important biological regulator and is a fundamental component in the fields of neuroscience, physiology, and immunology. Therefore, from the mentioned health

implication of nitrite and nitric oxide, there is need for their detection, quantification and detoxification in the environment using simple, effective and less expensive analytical techniques.

Many works on nitrite and nitric oxide determination using colourimetric and spectrophotometric methods have been reported [17-21]. These methods explored the potential of nitrite, nitric oxide and their oxidation products to form complexes with light absorbing groups in dyes and pigments, and the resulting changes in absorbance values measured as function of nitrite or nitric oxide concentration. Recently, electrochemical methods have also been demonstrated as simple, cost effective and convenient methods for nitrite and nitric oxide determination since it overrides draw-backs such as chemical derivatization and complex reaction procedure associated with conventional methods [14, 22-26]. However, electrochemical method requires some potential drive (voltage) to initiate the reaction between the catalyst and the analytes.

Thus, in this work, nickel oxide (NiO) and nickel hydroxide ($Ni(OH)_2$) nanoparticles were synthesized and the optimum chance for reactivity (without any voltage drive) which these nanoparticles would readily deliver, as against bulk materials was explored. This was done by simply mixing and stirring the catalyst and the analytes (NO_2^- and NO), and monitoring their catalytic effect on the oxidative degradation of these environmentally challenging molecules and by products of many industrial activities. The motivation to this work is (1) to synthesized NiO and $Ni(OH)_2$ in large quantity for commercial application on a large scale in waste water management and industrial effluent treatment plants. (2) to determine the ability, effectiveness and the efficiency of the synthesized materials to bring about the oxidation of these analytes at the possible minimum reaction time, devoid of chemical derivatization procedure or input of external voltage. The study showed that NiO nanopartilces gave better catalysis than $Ni(OH)_2$ towards NO_2^- and NO degradation, while NiO and $Ni(OH)_2$ at nano scale demonstrated enhanced catalysis towards the analytes compared with the bulk Ni salt. Since the production of NiO and $Ni(OH)_2$ nanoparticles requires simple preparation, therefore, a simple, portable, miniaturized nitrite and nitric oxide nanosensor can be fabricated from the materials.

2. MATERIALS AND REAGENTS

All chemicals and reagents used were of analytical grade and obtained from Sigma-Aldrich chemicals. They include, nickel chloride ($NiCl_2.6H_2O$), ammonium hydroxide (NH_4OH), ethanol, sodium nitrite ($NaNO_2$), disodium hydrogen phosphate ($Na_2HPO_4.2H_2O$), sodium dihydrogen phosphate ($NaH_2PO_4.2H_2O$) and hydrophoric acid (H_3PO_4). Phosphate buffer solution (PBS, pH 3.0 and 7.0) was prepared with appropriate amounts of H_3PO_4, $NaH_2PO_4.2H_2O$, and $Na_2HPO_4.2H_2O$ and the pH monitored with already calibrated pH meter. All solutions were prepared using freshly prepared distilled water.

All glassware, petri dishes, conical flasks and beakers used were washed in detergent solution, rinsed several times with distilled water and then soaked for 48 hours in 10 % HNO_3, after which they were rinsed further with distilled water and dried overnight in an oven at a temperature of 120 ^{o}C before used.

2.1 Synthesis of Nickel Hydroxide Ni(OH)₂ and Nickel Oxide (NiO) Nanoparticles

Synthesis of $Ni(OH)_2$ and NiO nanoparticles was carried out using the complexation-precipitation method with ammonium hydroxide as the complexing agent [27]. 100 mL of 2 M NH_4OH solution was added drop wise into 50 mL of 0.5 M $NiCl_2.6H_2O$ solution which was stirred by magnetic stirring apparatus at a constant temperature of 70 °C to give $Ni(OH)_2$ precipitate. The resultant light-green suspension was decanted, and then washed with water - ethanol solution at ratio of 1:1 for 5 to 10 times. It was then oven dried at 70 °C for 4 hrs to give $Ni(OH)_2$ nanoparticles. The synthesized $Ni(OH)_2$ nanoparticles is finally calcined at 800 – 900 °C for 4 – 5 hrs to give NiO nanoparticles. The synthesized $Ni(OH)_2$ and NiO were analysed using X-ray diffractometer (XRD minidifractomer, Radicon limited UK) with Cu $K_{\alpha}1$ radiation at 35 kV and 20 mA, with a scanning speed in 2 - 4 rev min $^{-1}$, field emission scanning electron microscopy, (FESEM) JEOL JSM 5800 LV, Japan) and a Fourier transformed infrared spectrometer (FTIR Nicolet iS5 Thermoscientific, UK) in the wavelength range of 400 to 4000 cm^{-1}. Catalysis experiment was carried out using UV-visible spectrophotometer (Helios Omega UV-Vis, Japan) in the absorbance range 200 – 700 nm.

2.2 Catalytic Experiment

Prior to the catalytic experiment, 10^{-3} M nitrite (NO_2^-) and 10^{-3} M nitric oxide (NO) were prepared by dissolving 0.0069 g of sodium nitrite ($NaNO_2$) in 100 mL of 0.1 M pH 7.4, and 0.1 M pH 3.0 phosphate buffer solutions (PBS) respectively. The catalytic experiment was carried out by introducing previously weighed 5 mg $Ni(OH)_2$ nanoparticles into a beaker containing 10 mL of 10^{-3} M NO_2^-. The mixture was continuously stirred for 5 mins and analyzed immediately using a UV visible spectrophotometer. The experiment was repeated using reaction time of 10 mins, 30 mins and 60 mins respectively. The absorbance reading was taken after each reaction time. Similar procedure was repeated for NO_2^- oxidation using NiO nanoparticles as catalyst. In the same vein, oxidation of 10^{-3} M NO was carried out using $Ni(OH)_2$ and NiO nanoparticles at different time as described for NO_2^- oxidation, and the absorbance values recorded. The effect of the bulk $NiCl_2$ in the catalytic oxidation of NO_2^- and NO was also investigated and compared with the nanoparticles.

3. RESULT AND DISCUSSION

3.1 Comparative XRD and FTIR analysis

The synthesised nanoparticles were characterized using powder X-ray diffractometer. Figure 1a shows the X-ray diffraction spectrum of $Ni(OH)_2$ nanoparticles sample. This shows a spectra structure with 8 major peaks. The XRD pattern shows a significant amount of line broadening indicating that the particles are nanocrystalline in nature with hexagonal phase. The synthesised $Ni(OH)_2$ sample spectrum correlates with the standard reference spectrum obtained by Wolff, 1972 [28] which is in good agreement with the standard pattern of $Ni(OH)_{2,}$ and spectrum reported for $Ni(OH)_2$ nanoparticles by Motlagh et al., 2011 [27], suggesting successful synthesis of $Ni(OH)_2$ nanoparticles. The XRD

pattern for Ni(OH)$_2$ also exhibits prominent peaks at 2θ values 18.96°, 32.78°, 38.29˚, 51.57˚ and 59.26° similar to that observed and reported for Ni(OH)$_2$ nanoparticles [27]. The crystal size was calculated according to Debye-Scherrer formula represented below (29, 30]:

$$D = 0.9\lambda \,/\, B\, Cos\Theta \quad .... (1)$$

Where wavelength of the radiations λ = 1.54 A˚, β is the full width at half maximum (FWMH), D = n = grain size, and θ is the angle obtained from 2θ values corresponding to maximum intensity peak in XRD pattern. From the equation, the mean crystal size of Ni(OH)$_2$ nanoparticle was calculated to be 5.07 nm.

On the other hand, the XRD spectrum of NiO nanoparticles (Fig. 1b) gave well define and resolved broad peaks indicating the crystalline nature of the nanoparticles, and also confirming the transformation of Ni(OH)$_2$ to NiO after calcining. The XRD internal library system confirms the compound to be NiO (Fig. 1b). The peaks gave corresponding 2θ values of 37.1°, 43.27° and 63.02°. The NiO sample spectrum correlates with the reference spectrum reported by Martin et al., 1991 [31] where the crystal was speculated to have cubic structure. The XRD pattern also agreed with that reported by Motlagh et al., 2011 [27] for nickel oxide nanoparticles. From Debye-Scherrer formula, the mean crystal size of NiO nanoparticle was estimated at 5.39 nm.
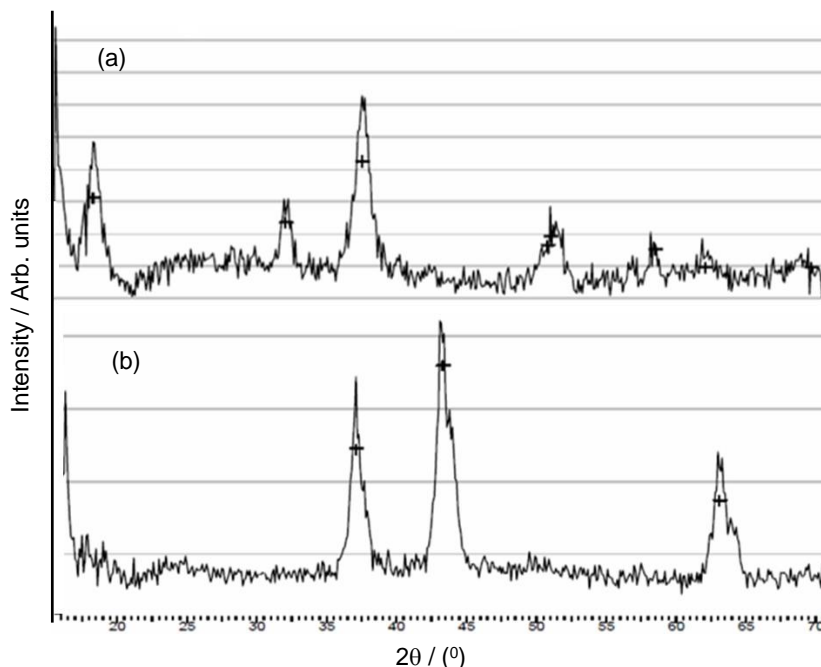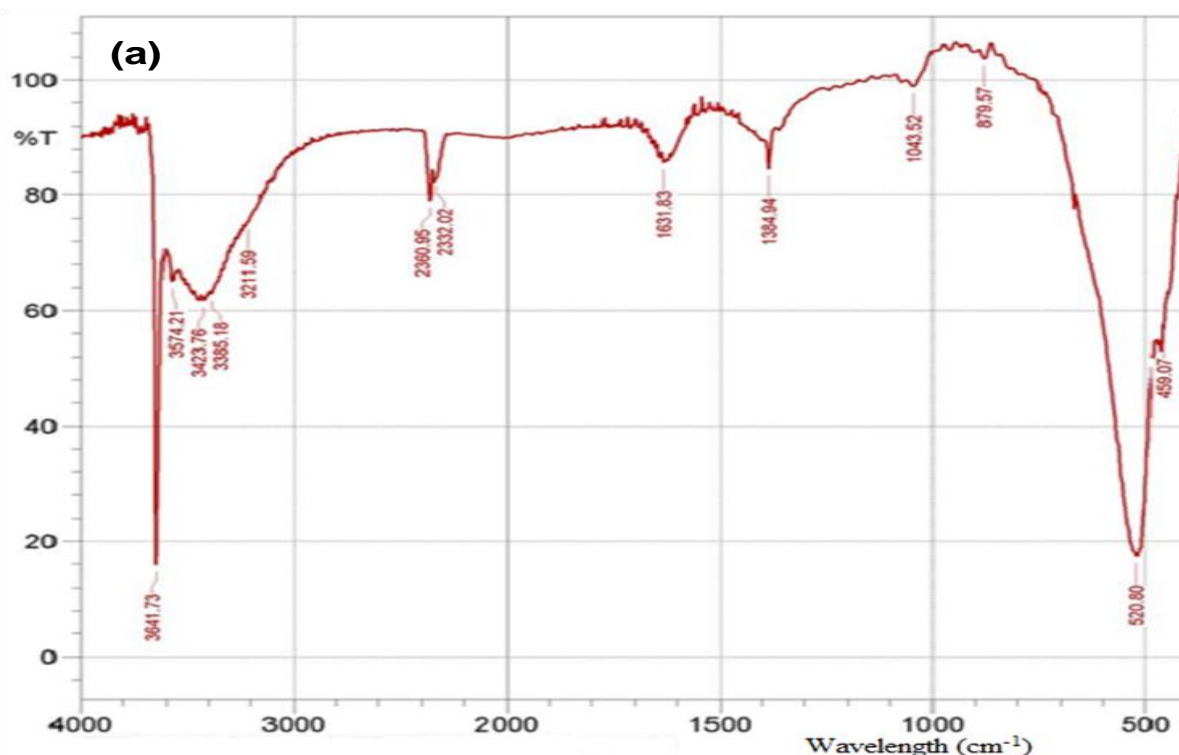

Figure 1. XRD spectra of the synthesised (a) Ni(OH)$_2$ and (b) NiO nanoparticles.

The FTIR spectrum of the Ni(OH)$_2$ nanoparticles is shown in Figure 2a. The FTIR spectrum shows the characteristics peaks at absorption bands 459.07, 520.8, 879.57, 1043.52, 1384.94, 1631.83, 2332.02, 2360.95, 3211.59, 3385.18, 3423.76, 3574.21 and 3641.73cm^{-1} respectively. The broad absorption band at around 3641.73cm^{-1} could be due to the O-H stretching vibrations, which is the characteristic of Ni(OH)$_2$ [27] and other OH containing compounds. The band at 1631.83 cm^{-1} can be

attributed to the bending vibration of water molecules or as a result of traces of N-H bond in the sample [32]. The band at 1384.94 cm^{-1} may be due to the presence of CO_3^{2-} anions from $Ni(OH)_2$ interaction with air [27]. The FTIR spectrum obtained for the NiO nanoparticles (Fig. 2b) shows different characteristics peaks from that of $Ni(OH)_2$ nanoparticles indicating successful transformation of $Ni(OH)_2$ to NiO after calcinations. The characteristic peaks are at absorption bands 435.93, 474.5, 875.71, 1045.45, 1384.94, 1433.16, 2359.02, 669.32, 1612.54, 2332.02 and 3444.98 cm^{-1} respectively. The appearance of new bands at 435.93cm^{-1} and 474.5 cm^{-1} in Figure 2b corresponds to the vibration of Ni-O bond. The band at 435.93cm^{-1} essentially reveals the presence of NiO [27]. Similarly, the prominence of the peaks at 1384.94, 1045.45, and the appearance of a new peak at 1433.16 cm^{-1} respectively in NiO spectrum over $Ni(OH)_2$ spectrum is a true reflection of structural transformation and formation of NiO nanoparticles. The drastic reduction in the intensity of the OH peak around 3641.73 cm^{-1} in $Ni(OH)_2$ to a reduced peak at 3444.98 cm^{-1} in NiO also confirmed the transformation of most of the OH groups to oxide. The bands at 3444.98 cm^{-1} and 1384.94 cm^{-1} could also be attributed to physically adsorbed OH (from water) and CO_3^{2-} groups on the calcined powders [27]. There is no peak indicating the presence of ammonia and chloride as the sample was washed with 50% ethanol. This shows that the sample contains little or no impurity.
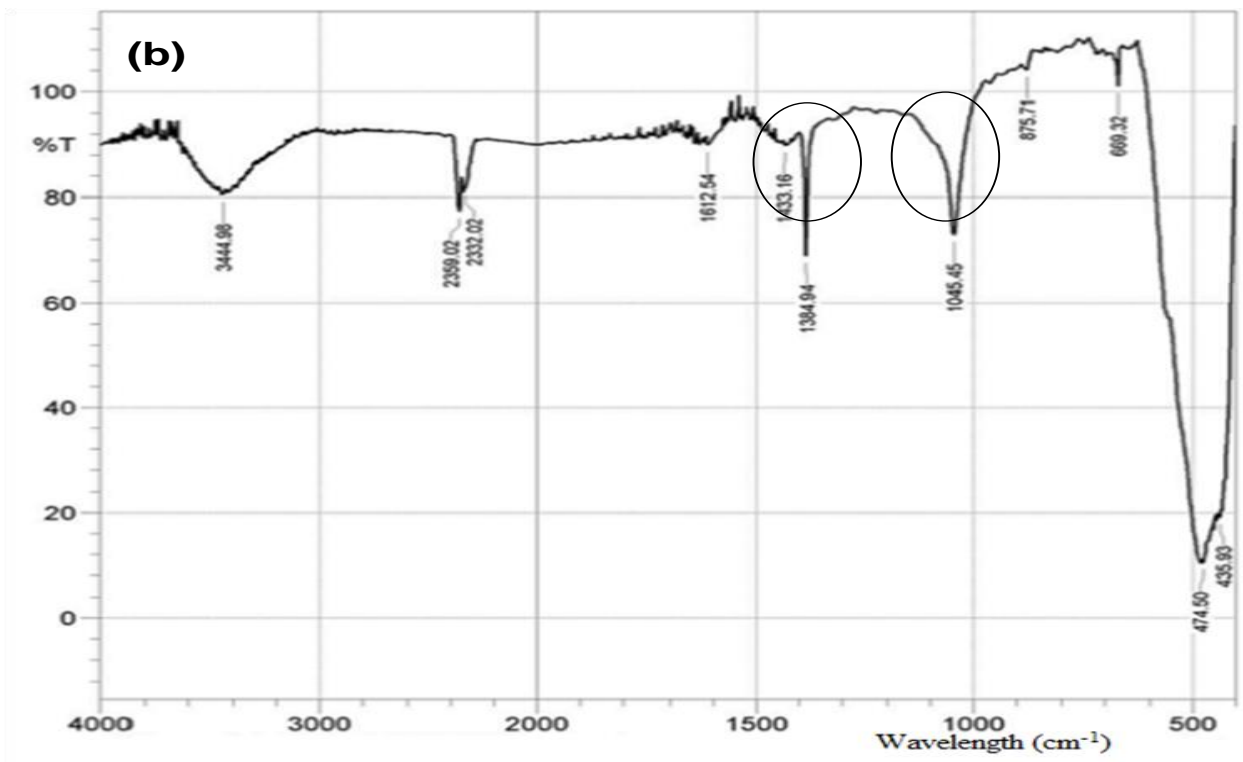
Figure 2. FTIR spectra of synthesised (a) Ni(OH)$_2$ and (b) NiO nanoparticles.

The field emission scanning electron microscopy (FESEM) image of the final calcined product (NiO) is presented in Figure 3. The NiO nanoparticles appeared crystalline and aggregated. From the SEM image, the average particle size is approximately 15 nm.
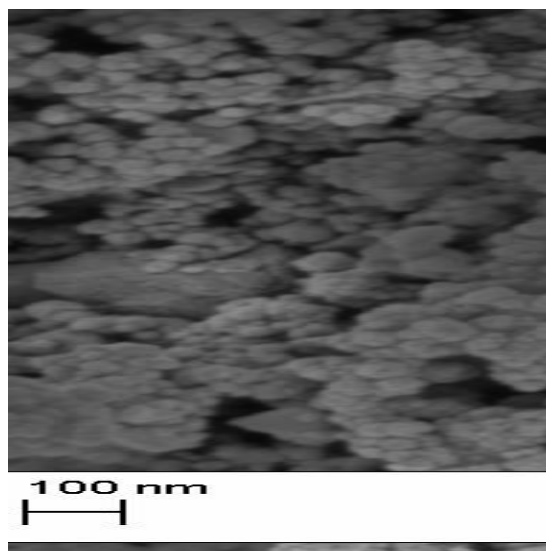

Figure 3. FESEM image of the calcined product, NiO nanoparticles.

3.2 Catalytic oxidation of NO_2^- and NO

The result of the catalytic oxidation of NO_2^- using $Ni(OH)_2$ nanoparticles is presented in Figures 4a and 4b. The experiment was performed by monitoring changes in absorbance as NiO and $Ni(OH)_2$ nanoparticles interact with NO_2^-. UV spectra were obtained in the absorbance range 200 – 700 nm. The experiment was carried out by taking the absorbance for the buffer alone, 10^{-3} M NO_2^-, and 10^{-3}M NO_2^- in the presence of $Ni(OH)_2$ at different reaction time. As expected, no peak was observed for the blank (buffer) solution. However, 10^{-3} M NO_2^- solution gave a peak at around 357 nm corresponding to NO_2^- absorption. Aside the NO_2^- peak at 357 nm, no other peak at higher wavelength was observed during the scan (see inset in Fig. 4a). However, in the presence of $Ni(OH)_2$ nanoparticles, the NO_2^- peak at 357 nm shifted slightly to lower λ max, with gradual increase in absorbance as the reaction time increased from 5 to 60 minutes. This indicate direct interaction between $Ni(OH)_2$ nanoparticles and NO_2^- molecules. The interaction did not bring about complete oxidation of NO_2^- to nitrate (NO_3^-) since no emergence of a new peak (nitrate peak) was observed, but the increase in absorbance with reaction time could be linked to the formation of light absorbing intermediates molecules which also absorb around 357 nm during NO_2^- oxidation. It was envisaged that if reaction time and $Ni(OH)_2$ catalyst loading for the oxidation process are increased, complete oxidation of nitrite to nitrate on the $Ni(OH)_2$ catalyst could be improved upon. NiO nanoparticles behaved differently towards nitrite catalysis (Fig. 4b). Upon addition of NiO nanoparticles to nitrite solution, a new absorption peak at lower wavelength (295 nm) corresponding to nitrate (NO_3^-) was observed for all the reaction time investigated. There had been report on UV detection of nitrate at approximately 290 nm and below [33].
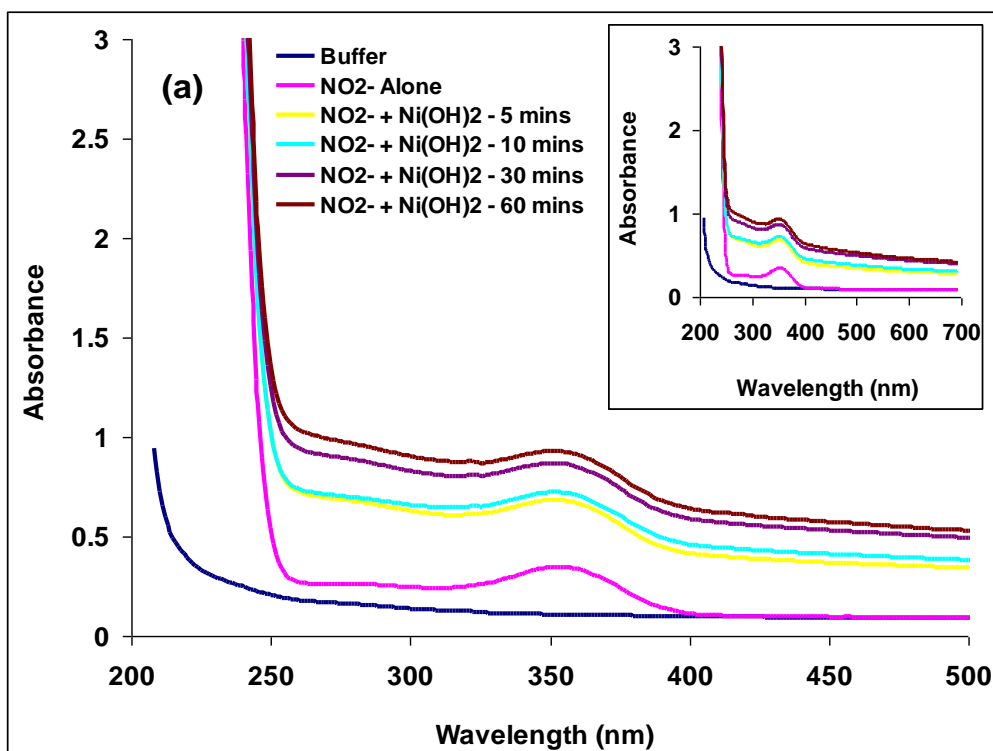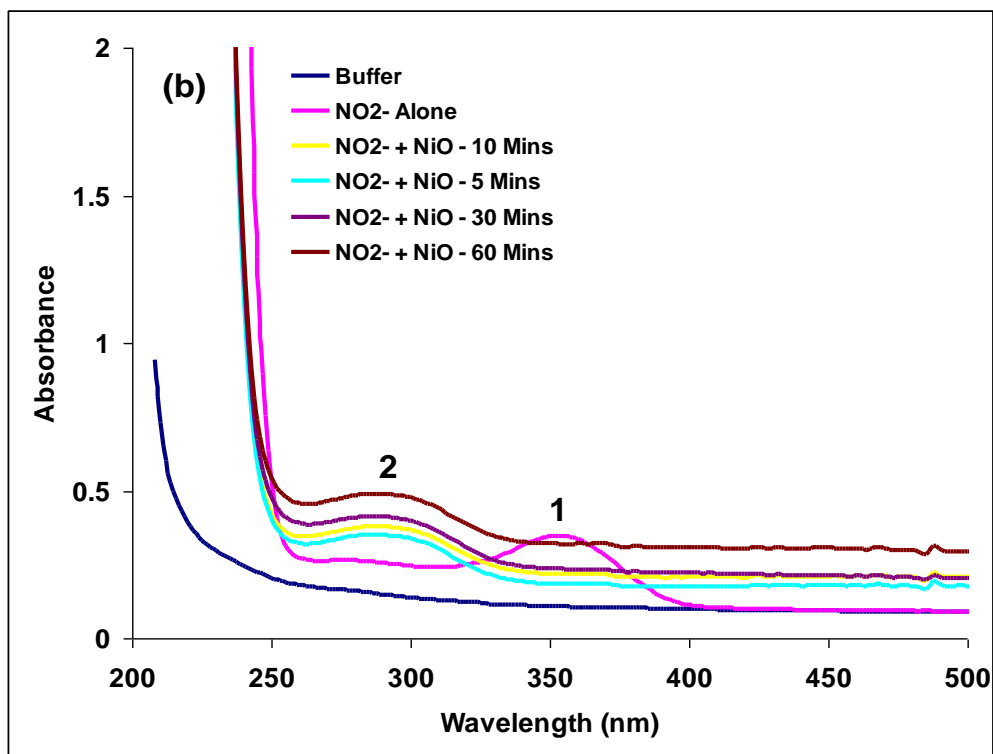
Figure 4. UV/Vis spectra showing the catalytic oxidation of 10^{-3} M NO_2^- using (a) $Ni(OH)_2$ nanoparticles and (b) NiO nanoparticles at different reaction time. Inset in (a) indicates that no peak was observed due to interference ions at higher wavelength.

The result obtained in this study therefore shows NiO nanoparticles as a better catalyst towards nitrite oxidative degradation and hence can be used for the treatment of municipal water and industrial effluents containing nitrite ion before final discharged into the environment and water bodies.

The result of the catalytic oxidation/degradation of 10^{-3} M NO using $Ni(OH)_2$ and NiO is presented in Figure 5. The oxidation experiment followed the same procedure as described for 10^{-3} M NO_2^- above. Figure 5a presents the UV-Vis spectra obtained for 10^{-3} M NO in the absence and presence of $Ni(OH)_2$. In the absence of $Ni(OH)_2$ nanoparticles, nitric oxide (NO) absorption peak was observed around 359-372 nm. In the presence of $Ni(OH)_2$ nanoparticles, there was significant increase in the absorbance at this same wavelengths for the reaction time of 5 and 10 minutes respectively. This result indicates that there is an interaction between the analyte and $Ni(OH)_2$ catalyst. Though no new peak was formed, it can be inferred that the increasing absorbance was contributed by oxidation intermediates formed during NO oxidation. The drop in the absorbance values for 30 and 60 minutes reaction time clearly suggest fouling effect or catalyst poisoning by the oxidation reaction intermediates. It could also mean that the NO molecules have been partly degraded to give their oxidation products which peaks are not visible enough probably due to interferences from un-oxidised nitric oxide (NO) molecules.
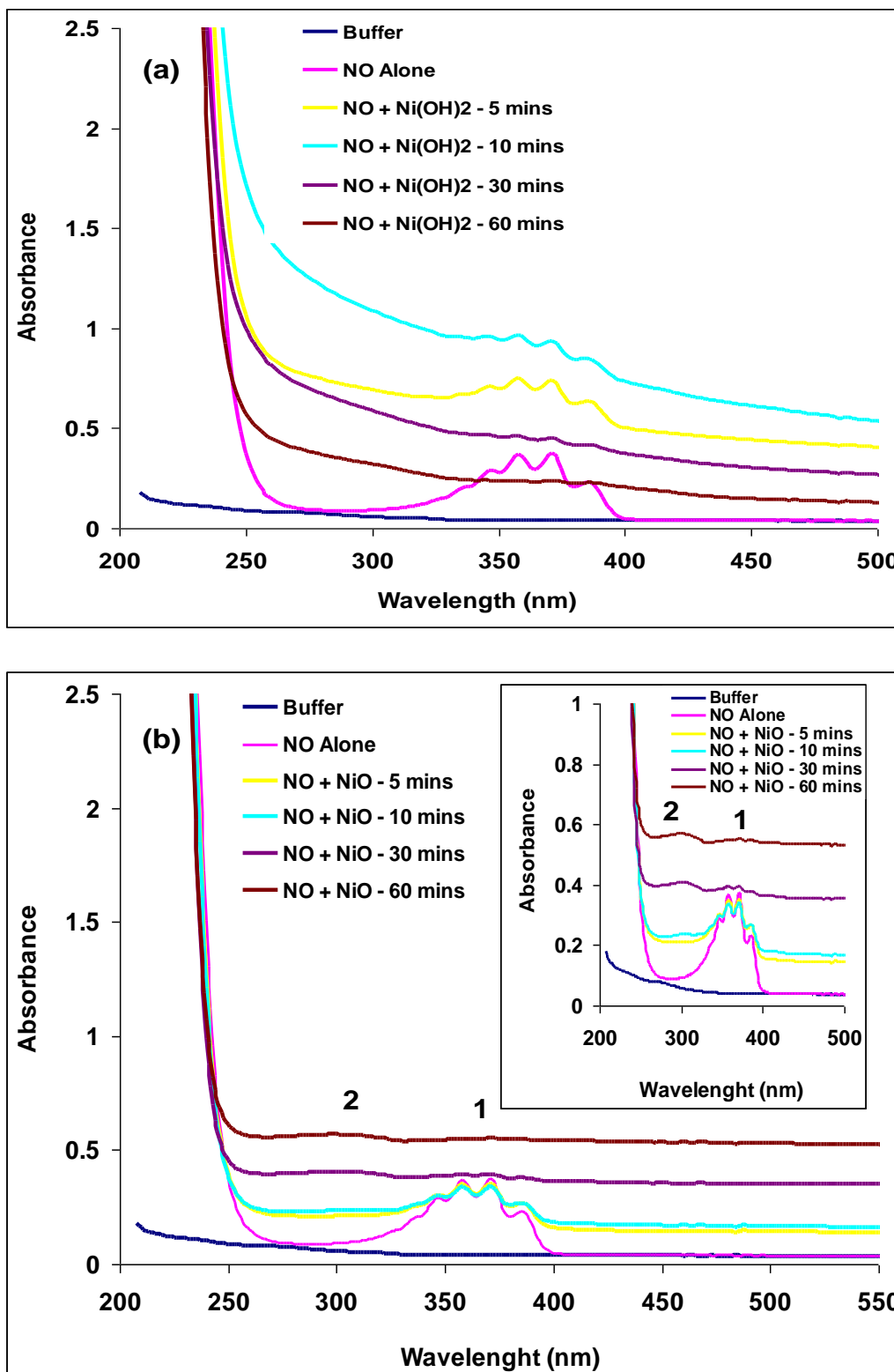
Figure 5. UV/Vis spectra showing the catalytic oxidation of 10^{-3} M NO using (a) Ni(OH)$_2$ nanoparticles and (b) NiO nanoparticles at different reaction time. Inset is modified form of (a) showing peak 2 due to NO$_3^-$ formation during oxidation.

Figure 5b presents the UV-Vis spectra obtained for 10^{-3} M NO in the absence and presence of NiO. It was observed that the presence of NiO in 10^{-3} M NO did not give any significant change in NO

absorbance peak (peak 1) for 5 and 10 minutes reaction time respectively except for a faint, small peak (peak 2) at 304 nm for 10 min reaction time. However, at longer reaction time (30 and 60 mins), a broad peak with increased absorbance intensity was observed (peak 1). At the same time, the small peak at around 304 nm became more obvious and shifted slightly to 307 nm (peak 2) (inset in Fig. 5b). Therefore, the result showed that there is an interaction between NO and NiO catalyst. The broad peak at 359-372 nm (peak 1) simply suggest gradual disappearance or conversion of NO to NO_3^-, thus, there is peak interference. The new small peak at 307 nm is attributed to the formation of NO_3^- molecules which is an oxidation product of NO. Formation of broad peak sometimes have been attributed to an overlap between an analyte (NO in this case) and its oxidation product (NO_3^- in this case), which probably was caused by slow and sluggish reaction kinetics. Therefore, a better and resolved peak separation can be achieved either by increasing NiO loading thereby creating more catalytic site for NO oxidation, or by providing more reaction time.

Figure 6 presents the catalytic effect of the bulk $NiCl_2$, the precursor salt used in the synthesis of $Ni(OH)_2$ and NiO nanoparticles. Presence of $NiCl_2$ in 10^{-3} M NO lead to reduction in NO peak at around 259-272 nm and the appearance of a new peak at 307 nm associated with formation of oxidation product (NO_3^-). However, the intensity of the nitrate (NO_3^-) peak obtained using NiO nanoparticles was five (5) times higher compared with the absorbance values obtained using bulk $NiCl_2$ as catalyst (Inset in Fig. 6). The result further underscores the catalytic efficiency of nanoparticles over bulk material in oxidation of nitrite and nitric oxide.
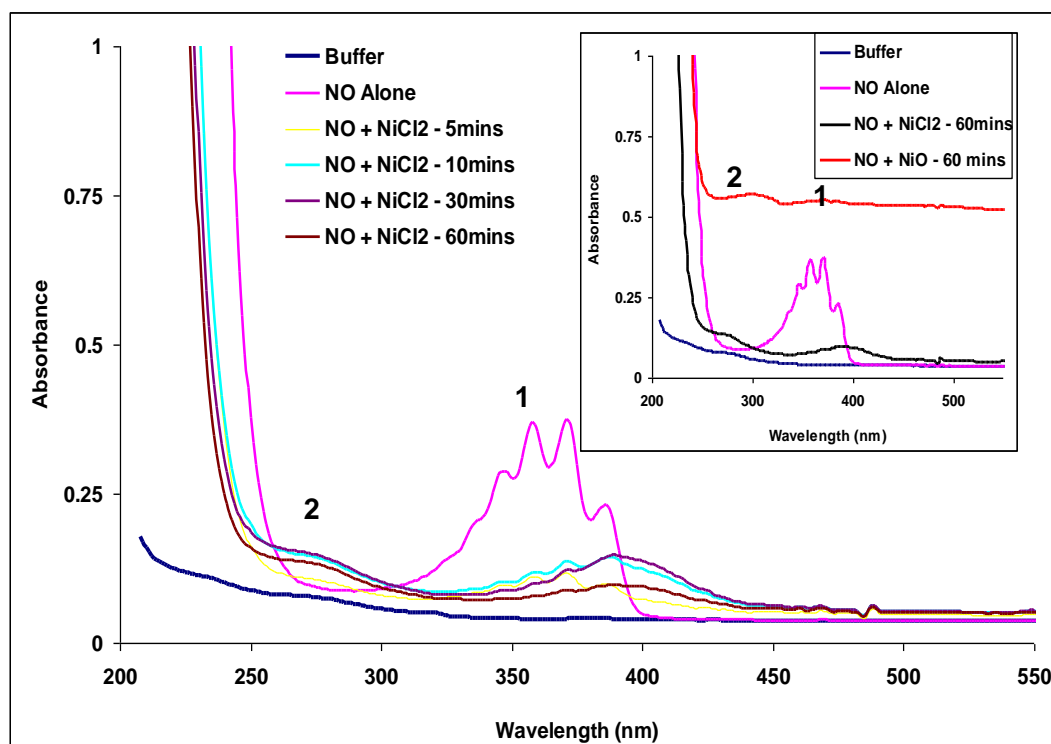

Figure 6. UV/Vis spectra showing the catalytic oxidation of 10^{-3} M NO using bulk $NiCl_2$. Inset in the figure presents the comparative UV/Vis Spectra obtained for the catalytic oxidation of NO using bulk $NiCl_2$ and NiO nanoparticles respectively at 60 mins reaction time.

Addition of NiCl$_2$ to 10^{-3} NO$_2^-$ did not give any observable or visible changes in the UV/Vis spectrum of NO$_2^-$ peak at 357 nm for every reaction time studied, suggesting that the NiCl$_2$ material is inactive or not catalytic in its bulk form towards NO$_2^-$ oxidation (Fig. 7). The only structural changes observed in the UV/Vis spectrum was an increase in absorbance at λ max 400 nm and above, for the reaction time 5 - 60 mins (Inset in Fig. 7). The reason for this dismal performance is not understood at the moment however, more detail work is ongoing to ascertain this.
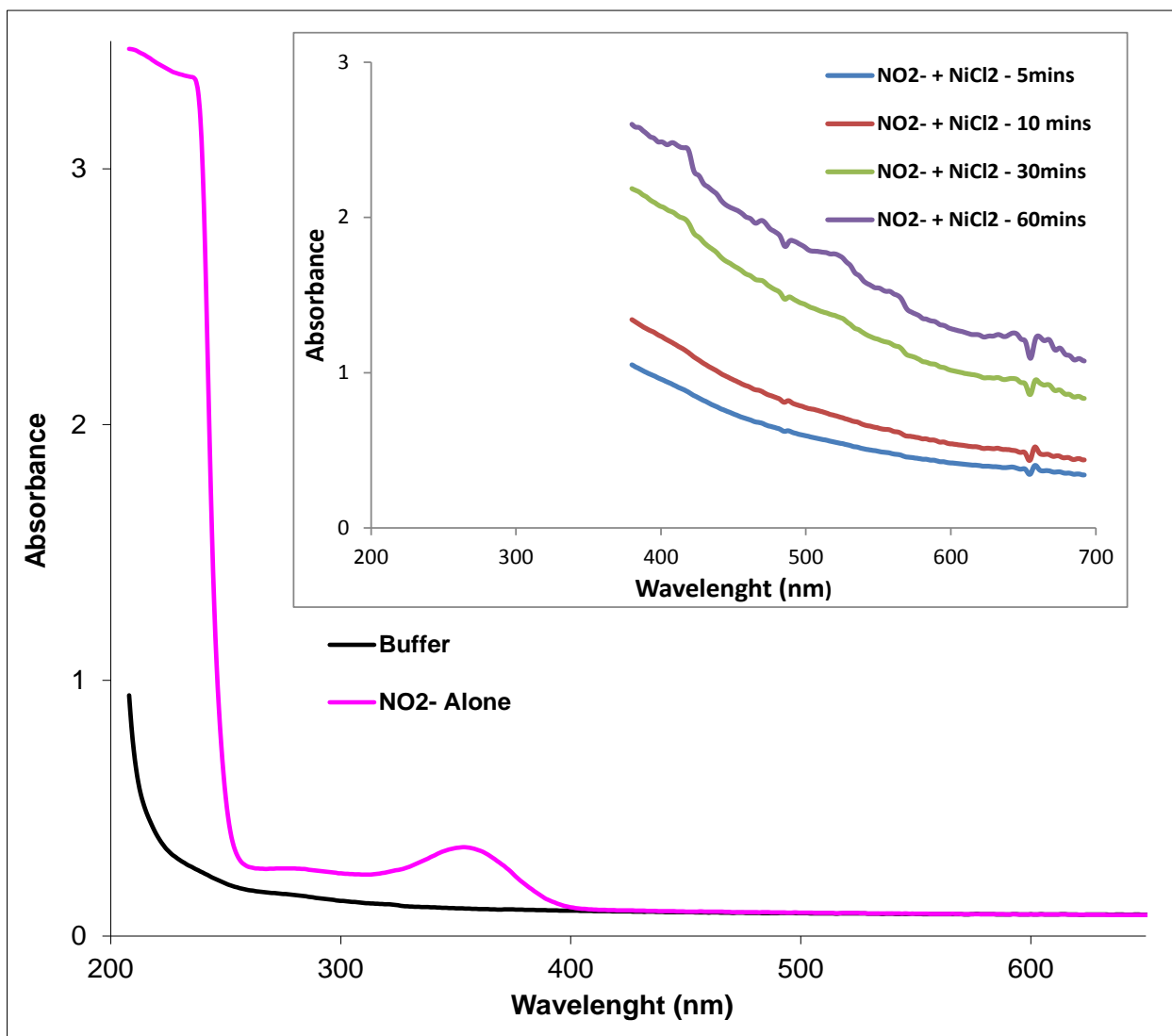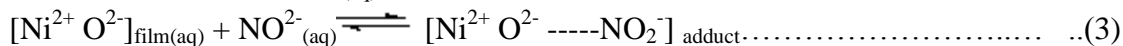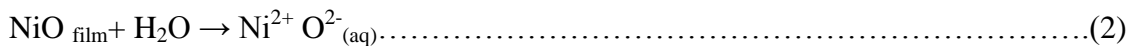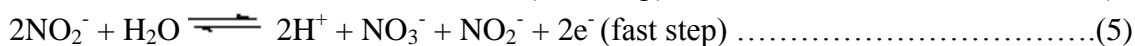

Figure 7. UV/Vis spectra representing NO$_2^-$degradation using bulk NiCl$_2$ at different reaction time.

Thus, the improve catalytic properties of the synthesized Ni(OH)$_2$ and NiO nanoparticles used in this work over bulk NiCl$_2$ could be due to the effective pore sizes and large surface area of nanoparticles which expose the analytes to more catalytic site than is obtained on the bulk material. Also, at nano size levels, there is easy flow and exchange of electrons between analyte and the nanoparticles leading to enhanced reaction mechanism. Based on the result obtained in this study and

related study on nitrite and nitrate oxidation [34], the mechanism below was assumed for the catalytic oxidation of nitrite in the presence of NiO nanoparticles.

$$NiO_{film} + H_2O \rightarrow Ni^{2+} O^{2-}_{(aq)} \dots\dots\dots\dots\dots\dots\dots\dots\dots\dots\dots\dots\dots\dots\dots\dots (2)$$

$$[Ni^{2+} O^{2-}]_{film(aq)} + NO^{2-}_{(aq)} \rightleftharpoons [Ni^{2+} O^{2-} \text{-----}NO_2^-]_{adduct} \dots\dots\dots\dots\dots\dots\dots\dots.. ..(3)$$

$$\text{Catalyst} - \text{substrate overlap}$$

$$[Ni^{2+} O^{2-} \text{-----}NO_2^-]_{adduct} \rightarrow NiO + NO_2^- \text{ (slow step)} \dots\dots\dots\dots\dots\dots\dots\dots\dots.(4)$$

$$2NO_2^- + H_2O \rightleftharpoons 2H^+ + NO_3^- + NO_2^- + 2e^- \text{ (fast step)} \dots\dots\dots\dots\dots\dots\dots\dots(5)$$

$$NO_2^- + H_2O \rightarrow 2H^+ + NO_3^- + 2e^- \dots\dots\dots\dots\dots\dots\dots\dots\dots\dots\dots\dots\dots\dots \dots(6)$$
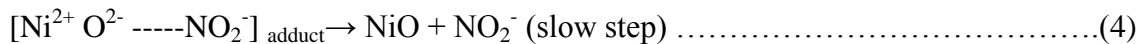
In Phosphate Buffer Solution, NiO film ionizes forming $Ni^{2+} O^{2-}$ as shown in equation 2. Nitrite ion interacts with the $Ni^{2+} O^{2-}$ions forming adduct (Eqn 3). Equation 4 represents the rate determining step which is a one-electron process involving formation of an intermediate product (NO_2^-). Formation of NO_2^- is followed by its disproportionation to give nitrate and nitrite (Eqn 5). The nitrite is further oxidized to give more nitrate product (Eqn 6).

4. CONCLUSION

The present study has demonstrated that the complexation-precipitation method is an effective method of preparing Nickel oxide (NiO) and Nickel Hydroxide ($Ni(OH)_2$) nanoparticles of high purity with ultra-fine particle sizes of 5.39 nm and 5.07 nm respectively as confirmed by the XRD and the FTIR results. The catalytic properties of both Nickel oxide (NiO) and Nickel Hydroxide ($Ni(OH)_2$) nanoparticles towards degradation of NO_2^- and NO to nitrate (NO_3^-) were also confirmed using UV-vis spectroscopic technique. The two synthesized nanoparticles demonstrated enhanced catalysis towards the analytes studied compared with the activities of their precursor or bulk material ($NiCl_2$). The results from the study indicate that NiO nanoparticles is a better catalyst towards nitrite and nitric oxide oxidative degradation than $Ni(OH)_2$ nanoparticles. Increased reaction time also favoured the reaction mechanism, and hence, better catalysis. The bulk $NiCl_2$ material has no observable catalytic oxidative effect on NO_2^-, but produced a new peak in NO, associated with NO_3^- formation. The new peak intensity was five times lower than that obtained in NO using NiO nanoparticles. The study therefore indicates the significance of nanosynthesised material over their bulk counterpart in catalysis.

References

1. A. Abbaspour, A. Khajehzadeh, A. Ghaffarinejad, *J. Electrochem.*, 631 (2009) 52.

2. A. Mohammadi, A.B. Moghaddam, M. Kazemzad, R. Dinarvand, J. Badraghi, *Mater. Sci. and Eng., C*, 29 (2009) 1752.
3. A. Salimi, A. Noorbakhash, E. Sharifi, A. Semnani, *Biosensors and Bioelectronics*, 24 (2008) 792.
4. J. Li, E. Liu,W. Li, X. Meng, S. Tan, 478 (2009) 371.
5. Z. Zheng, L. Huang, Y. Zhou, X. Hu, X. Ni, *Solid State Sciences*, 11(2009) 1439
6. V. Gupta, T. Kawaguchi, N. Miura, *Mater. Res. Bull.*, 44 (2009) 202.
7. S. B. Colin, *J. of Mater.l Sci.*, 338 (2002) 70.
8. A.N. Shipway, E. Katz, I. Willner, "Nanoparticle Arrays On Surfaces for Electronic, Optical, and Sensor Applications. Phy. Chem., First Edition, pp. 18–52, 2000.
9. Y. Min,Y. Chen, Y. Zhao, C. Chen, *Mater. Lett.*, 62 (2008) 4503.
10. T. Stimpfling, F. Leroux, *Chem Mater.*, 22 (2010) 974.
11. M. Vidotti, R.P. Salvador, S.I. Córdoba de Torresi, *Ultrasonics Sonochemistry*, 16 (2009) 35.
12. A. Pacuła, P. Nowak, R.P. Socha, M. Ruggiero-Mikołajczyk, D. Mucha, E. Bielanska, *Electrochim. Acta*, 90 (2013) 563.
13. M. Vidotti, M.R. Silva, R.P. Salvador, S.I. Cordoba Torresi, L.H. Dall'Antonia, *Electrochim. Acta*, 53 (2008) 4030.
14. A.S. Adekunle, B.B. Mamba, B.O. Agboola, K.I. Ozoemena, *Int. J. Electrochem. Sci.,* 6 (2011) 4388.
15. M.W. Lomas, F. Lipschultz, *Limnology and Oceanography*, 51 (2006) 2453.
16. J.L. Sarmiento, C. LeQuere, Science, 274 (1996) 1346.
17. A.D. Beaton, V. J. Sieben, C. F.A. Floquet, E. M. Waugh, S.A.K. Bey, I. R.G. Ogilvie, M. C. Mowlem, H. Morgan, *Sensors and Actuators B*, 156 (2011) 1009.
18. E.T. Steimle, E. A. Kaltenbacher, R. H. Byrne, *Marine Chem.*, 77 (2002) 255.
19. X-F. Yue, Z-Q. Zhang, H-T. Yan, *Talanta*, 62 (2004) 97.
20. R. Andradea, C. O.Viana, S.G. Guadagnin, elix G.R. Reyesb, S. Rath, *Analytical, Nutritional and Clinical Methods, Food Chemistry*, 80 (2003) 597.
21. N. A. Zatar , M.A. Abu-Eid, A. F. Eid, *Talanta*, 50 (1999) 819.
22. A.S. Adekunle, J. Pillay, K.I. Ozoemena, *Electrochim. Acta*, 55 (2010) 4319.
23. A.S. Adekunle, K. I. Ozoemena, *Electroanalysis*, 22 (2010) 2519.
24. P. Tau, T. Nyokong, *Electrochim. Acta* 52 (2007) 4547.
25. F. Matemadombo, T. Nyokong, *Electrochim. Acta* 52 (2007) 6856.
26. B.O. Agboola, T. Nyokong, *Anal. Chim. Acta* 587 (2007) 116.
27. M. Motlagh, M. Kashani, A. Youzbashi A., SabaghzadehL, *Int. J. Phy. Sci.,* 6 (2011) 1471.
28. De P. Wolff, Technisch PhysischeDienst,Delft, Netherlands, 1972.
29. Y-K. Sun, M. Ma, Y. Zhang, N. Gu, *Coll. Surf. A: Physicochem Eng Aspects*, 245(2004) 15.
30. R.M. Cornell, U. Schertmann, "Iron Oxides in the laboratory: Preparation and Characterization", VCH, Weinheim, 1991.
31. K. Martin, G. McCarthy, North Dakota State University, Fargo, ND, USA. Winchell, Winchell, 1991.
32. P. Gans, "Vibrating Molecules: an Introduction to the Interpretation of Infrared and Raman Spectra", Chapter 3, pp. 117 – 120, 1975.
33. M. Lookabaugh, I. S. Krull, *J. Chromatography,* 452 (1988) 295.
34. F. Armijo, M.C. Goya, M. Reina, M.J. Canales, M.C. Arevalo, M.J. Aguire, *J. Mol. Catal. A* 268 (2007) 148.